Available online at www.sciencedirect.com
SCIENCE DIRECT®
Physics and Chemistry of the Earth 30 (2005) 1030–1037
PHYSICS and CHEMISTRY of the EARTH
www.elsevier.com/locate/pce

# Mobility of U–Th radionuclides connected with fault porosity: A case study of the Schauenburg Fault, Rhine Graben Shoulder, Germany

Thierry Marbach [a,*], Bernd Kober [b,1], Augusto Mangini [c,2], Laurence Warr [d,3], Anja Schleicher [e,4]

[a] Institute of Environmental Physics, INF 229, 69120 Heidelberg, Germany
[b] Institute of Environmental Geochemistry, INF 236, 69120 Heidelberg, Germany
[c] Heidelberg Academy of Sciences, INF 229, 69120 Heidelberg, Germany
[d] Centre de Géochimie de la Surface (CNRS-ULP), 1 rue Blessig, 67084-Strasbourg, France
[e] Geologisch-Paläontologisches Institut, Ruprecht-Karls-Universität, INF 234, 69120 Heidelberg, Germany

Received 21 March 2004; received in revised form 11 February 2005; accepted 17 February 2005

**Abstract**

This study focuses on the relationship between U- and Th-isotope distribution, and the porosity/permeability structure of a geological fault in the uplifted Rhine Graben shoulder (SW-Germany). This fault, known as the Schauenburg Fault, separates basement Variscan granite from Permian rhyolite, and is marked by a clay-bearing cataclasite. All fault rock samples are characterized by the redistribution of uranium and thorium isotopes within the last $\sim 10^6$ years, whereas in the granite and the rhyolite only uranium isotopes leaching (activity ratio <1) has occurred. The cataclasite samples, with $^{234}U/^{238}U > 1$, record a complex history of sorption and loss of uranium isotopes. The uranium activity ratios are higher for the samples collected close to the fault plane and lower for cataclastically deformed fault rock situated away from the principal displacement surface. The porosity measurements of the cataclasite show symmetrical variations across the core of the fault zone, similar to the pattern of uranium activity ratios. In order to relate the porosity data with the $\delta^{234}U$ value, a simple exchange model was developed assuming that the change in the uranium activity ratios results from uranium isotopic exchange with the aqueous phase. Best approximations were obtained by using an isotopic water/rock exchange coefficient for $^{234}U$ ranging from 2.5E−06 [$a^{-1}$] in the core of the fault zone to 2.5E−05 [$a^{-1}$] for the fault walls, whereby the isotopic water/rock exchange per year is the same dimension as the radioactive decay constant. Along the outer core of the fault zone, the increased porosity, and thus permeability, resulted in prolonged contact between water and rock. Here, a higher isotopic exchange of uranium with the aqueous phase has occurred. Within the core of the fault, the porosity is lower and the availability of circulating fluids restricted the exchange of uranium isotopes between the rock and the aqueous phase. The resulting exchange time for the isotopic exchange coefficient is 70 ka, which suggests a young fluid–rock interaction event possibly related to the last stage of Rhine graben fault activity along this structure.


*Keywords:* U–Th radionuclides; Granite; Fault zone; Porosity; Water–rock interaction; Exchange model

## 1. Introduction

Quantifying the changes in composition and concentration of radiogenic isotopic elements in the Earth's crust that occur during fluid–rock interaction are essential to our understanding of crustal processes, for the exploration of mineral deposits, and for the safer disposal of nuclear waste materials in underground repositories. In the upper portion of the crust, faults constitute the principal sites of high

* Corresponding author. Tel./fax: +49 6221 54 6405.
*E-mail addresses:* mthierry@iup.uni-heidelberg.de (T. Marbach), bernd.kober@urz.uni-heidelberg.de (B. Kober), amangini@iup.uni-heidelberg.de (A. Mangini), warr@illite.u-strasbg.fr (L. Warr), aschleic@ix.urz.uni-heidelberg.de (A. Schleicher).
[1] Fax: +49 6221 54 4956.
[2] Fax: +49 6221 54 6405.
[3] Fax: +333 88 36 72 35.
[4] Fax: +49 6221 54 5503.

1474-7065/$ - see front matter © 2005 Elsevier Ltd. All rights reserved.
doi:10.1016/j.pce.2005.02.001

fracture permeability, where the chemical impact of fluid–rock interaction can be observed on a variety of scales (microscopic to several meters). In most natural faults, the permeability and porosity structure of cataclastically formed fault rocks can be largely related to fault activity. Studies of tectonically active terrains have shown that fault displacements in the upper continental crust are largely accomplished by increments of seismic slip along pre-existing structures (Sibson, 1994). In the vicinity of faults that undergo intermittent rupturing, variations in permeability and fluid flux are considered to be intimately related to the earthquake cycle and stress cycling (Chester et al., 1993; Sibson, 1994). The intrinsic roughness and interconnection of natural fault surfaces (Power et al., 1987) has the implication that freshly ruptured faults should become highly permeable pathways for fluid flow. During the longer interseismic periods, faults often develop impermeable seals by the formation of clay-rich gouge and hydrothermal cements (Smith, 1980; Hooper, 1991; Vrolijk and van der Pluijm, 1999). Evidence from geothermal fields suggests that hydrothermal flow along fractures rapidly leads to hydrothermal precipitation and self-sealing (Batzle and Simmons, 1977). Thus in fault zones, a range of processes and resulting materials could be expected, possibly leading to an increase or decrease in fracture permeability (Caine et al., 1996).

This study addresses the behaviour of U- and Th-isotopes during fluid–rock interaction and its relationship with the porosity/permeability structure of a rift-related fault of the Rhine Graben, Germany. The U–Th isotopic signatures across the fault zone reflect a conduit-barrier type fault, characterized by a relatively impermeable fault core acting as a barrier, and highly fractured wall-rock forming zones of preferential fluid flow. Based on these isotopic signatures, we evaluate the Th/U dating method on a system perturbed by uranium isotopic exchange, and estimate the extent and timing of recent alteration attributable to the downward flow of meteoric waters and possibly to fault reactivation.

## 2. Geological setting

The studied area is located along the eastern Rhine Graben shoulder, in the southern part of the Variscan crystalline Odenwald (SW-Germany), close to Heidelberg. Lying just 100 m east of the N–S trending Rhine Graben bounding fault, the Variscan "Heidelberger Granite" is faulted against Permian rhyolite across the steeply dipping E–W trending Schauenburg fault (Fig. 1). The fault, which was temporarily exposed during archeological trenching, provides a good opportunity to investigate fluid–rock-interaction processes associated with brittle deformation along the uplifted shoulders of the Rhine graben rift system. For the granite, Hess and Lippolt (1996) recorded well defined $^{40}Ar/^{39}Ar$ ages of $332 \pm 3$ and $328 \pm 1$ Ma ($2\sigma$ errors), obtained on hornblendes and sericite-free plagioclase, confirming earlier K–Ar and Ar–Ar ages of around 335 Ma (Lippolt et al., 1990). For the rhyolite, $^{40}Ar/^{39}Ar$ measurements of sanidine, biotite and muscovite, indicate a Permo-Carboniferous age

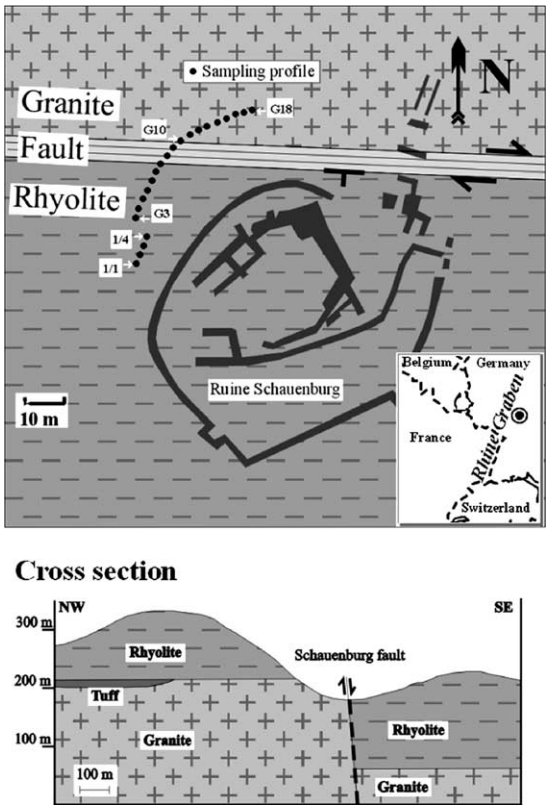


Fig. 1. This figure shows both a map of the working area with the sampling profile (above) and a cross-section on a greater scale of the same area (below). The Schauenburg fault zone is located along the eastern Rhine Graben shoulder, in the southern part of the Variscan crystalline Odenwald (SW-Germany), close to Heidelberg. This E–W trending oblique-slip fault is situated perpendicular to the main NNE–SSW Rhine Graben fault, and runs through the Schauenburg castle trench. Samples (22 in total) with varying degree of alteration were collected across the fault zone at 1 m intervals.

($291 \pm 6$ Ma $2\sigma$ errors; Lippolt et al., 1990), indicating a ca. 40 Ma age difference between Carboniferous plutonism and the later rhyolitic volcanism for this locality.

The 800 m long, E–W trending, Schauenburg fault is situated perpendicular to the main NNE–SSW Rhine Graben fault, and runs through the Schauenburg castle trench (Fig. 1). Geological mapping of the fault reveals an oblique dextral strike-slip displacement of ca. 100 m, with a downthrow to the south (Schleicher, 2001). A total of 22 samples has been collected across the fault zone at 1 m intervals. Macroscopic features reveal varying degrees of alteration of the samples, with the fault plane marked by the occurrence of a clay-rich cataclasite.

## 3. Sample description and analytical methods

Based on macroscopic and petrographic observations, three zones and sample groups can be recognized across the sampling profile.

Fractured, fine-grained rhyolite: samples 1/1 to 1/4.

Strongly altered clay-bearing cataclasite: samples G3–G11.

Intensely fractured and altered granite, with large alkali-feldspars, quartz and biotite: samples G12 to G18.

The mineral assemblages of the study material, described in detail by Schleicher (2001) and Schleicher et al. (2005), can be is summarized as follows. The primary minerals of the granite and the rhyolite rock types are quartz, K-feldspar, plagioclase and biotite, with secondary illite, illite-smectite mixed-layered phases, kaolinite and occasional discrete smectite characterizing the clay-sized fraction. Accessory minerals are typically hematite and rutile, with some apatite and calcite. The most altered samples are those of the clay-rich cataclasite collected along the trace of the fault. These samples are enriched in illite-smectite and kaolinite minerals formed during retrograde reactions within the fault zone (Schleicher et al., 2005).

For analytical investigations, samples were crushed, the external parts of the samples exposed to meteoritic alteration removed and the remaining rock chips powdered. As uranium is a very leachable element (Ivanovich and Harmon, 1992), mineralogical separation, isotopic and chemical analyses were performed on whole rock samples without contact with water at any stage of the sample preparation. Powdered samples were dissolved with a suprapur concentrated HF/HCl/$HNO_3$ mixture (1:1:3 by volume). A $^{229}$Th spike and $^{233}$U/$^{236}$U double spike were added for concentration determinations. The $^{229}$Th spike was calibrated against the internal HDAKT-1 $^{232}$Th standard. The concentration of the $^{233}$U/$^{236}$U double spike was calibrated against the NIST CRM 960 uranium standard. Methodology for the $^{233}$U/$^{236}$U double spike and the $^{229}$Th spike are described in Bollhöfer et al. (1996) and Frank (1997). Dissolution was carried out in closed, pressurized teflon bombs placed in a microwave oven (15 bars and 110 °C during 1 h). The separation and purification of thorium and uranium were made using anion exchange procedures with $HNO_3$ and HBr as eluants. Isotopic measurements were performed using a FINNIGAN MAT 262 thermal ionization mass spectrometer (TIMS) equipped with a retarding potential quadrupole (RPQ). Uranium was determined with a single electron multiplier ($^{233}$U, 234U, $^{235}$U and $^{236}$U) and 1 faraday cup ($^{238}$U). The natural ratio of $^{235}$U/$^{238}$U was used to calibrate the yield of the multiplier. The peak flatness is better than 0.2% (over 150 ppm in mass). The $\delta^{234}$U of the NIST CRM 960 uranium standard was measured at $-31.8 \pm 4.1$ [‰], in good agreement with Chen et al. (1986), Edwards et al. (1993), Eisenhauer et al. (1993), and Sturchio (1994). The reproducibility of the isotopic ratio of $^{234}$U/$^{238}$U during the period of the measurements was 0.6% ($2\sigma$). $^{238}$U and $^{232}$Th blanks were routinely measured and used for blank corrections. The blank averages are 3 ng for $^{238}$U and 0.7 ng for $^{232}$Th. The analytical procedures of the sample preparation and data acquisition by TIMS measurements are detailed in Bollhöfer et al. (1996) and Marbach (2002).

The porosity of the samples were measured by mercury injection porosimetry at the Centre de Géochimie de la Surface in Strasbourg using the methodology of Surma and Géraud (2003).

Table 1
Sampling profile of Th and U across the fault zone

| | Sample | Distance between samples [m] | $^{234}$U/$^{238}$U activity ratio | Error abs. | $\delta^{234}$U [‰] | Error abs. | $^{238}$U [ppm] | Error abs. | $^{230}Th_{exc}$ [dpm/g] | Error abs. | Porosity [%] |
|---|---|---|---|---|---|---|---|---|---|---|---|
| Rhyolite | 1/1 | 0 | 0.894 | 0.004 | −106 | 4 | 7.188 | 0.019 | 1.91 | 0.14 | |
| | 1/2 | 1 | 0.910 | 0.004 | −90 | 4 | 6.027 | 0.012 | 1.19 | 0.08 | |
| | 1/3 | 2 | 0.921 | 0.007 | −79 | 7 | 5.094 | 0.010 | 2.18 | 0.17 | |
| | 1/4 | 3 | 0.899 | 0.003 | −101 | 3 | 5.721 | 0.008 | 0.65 | 0.07 | |
| | G3 | 4 | 0.931 | 0.010 | −69 | 10 | 3.060 | 0.011 | 1.21 | 0.09 | 6.68 |
| Cataclasite | G4 | 5 | 1.158 | 0.008 | 158 | 8 | 4.947 | 0.023 | 0.83 | 0.12 | |
| | G4b | 6 | 1.086 | 0.013 | 86 | 13 | 3.775 | 0.020 | 0.76 | 0.10 | 8.38 |
| | G5 | 7 | 1.061 | 0.011 | 61 | 11 | 3.485 | 0.016 | 0.71 | 0.09 | 7.44 |
| | G6 | 8 | 0.998 | 0.006 | −2 | 6 | 4.625 | 0.014 | 0.70 | 0.06 | 7.23 |
| | G7 | 9 | 1.021 | 0.013 | 21 | 13 | 2.933 | 0.011 | 3.18 | 0.10 | |
| | G8b | 10 | 0.989 | 0.013 | −11 | 13 | 1.599 | 0.005 | 0.49 | 0.05 | 3.51 |
| | G8c | 11 | 0.957 | 0.007 | −43 | 7 | 4.954 | 0.019 | 0.35 | 0.07 | |
| | G9 | 12 | 1.020 | 0.013 | 20 | 13 | 1.999 | 0.012 | 0.26 | 0.03 | 6.84 |
| | G10 | 13 | 1.095 | 0.003 | 95 | 3 | 2.064 | 0.003 | 0.44 | 0.03 | 13.43 |
| Granite | G11 | 14 | 0.973 | 0.003 | −27 | 3 | 2.570 | 0.002 | 0.44 | 0.02 | 8.18 |
| | G12 | 15 | 0.923 | 0.007 | −77 | 7 | 3.037 | 0.008 | 0.68 | 0.06 | |
| | G13 | 16 | 0.905 | 0.003 | −95 | 3 | 3.215 | 0.005 | 0.49 | 0.05 | 4.87 |
| | G14 | 17 | 0.885 | 0.008 | −115 | 8 | 1.754 | 0.004 | 0.79 | 0.05 | 3.6 |
| | G15 | 18 | 0.960 | 0.007 | −40 | 7 | 3.335 | 0.010 | 1.45 | 0.13 | |
| | G16 | 19 | 0.937 | 0.004 | −63 | 4 | 4.631 | 0.012 | 0.52 | 0.06 | |
| | G17 | 20 | 0.937 | 0.004 | −63 | 4 | 2.529 | 0.004 | 0.57 | 0.04 | |
| | G18 | 21 | 0.967 | 0.003 | −33 | 3 | 2.659 | 0.004 | 0.77 | 0.07 | |

$\delta^{234}U = (([^{234}U/^{238}U] - 1) \times 1000))$ (activities). $^{230}Th_{exc} = ^{230}Th - ^{234}U$ (activities). The uncertainties are $\pm 2\sigma$ for the uranium and thorium data. The error for the porosity is 4%.

## 4. Results

The uranium and thorium contents (Table 1) of the samples correspond well with published data on granite and rhyolite from other areas (Rogers and Adams, 1969; Kaufman et al., 1971; Harmon et al., 1975; Kunzendorf and Friedrich, 1976). The results show characteristic signatures for the three defined zones (rhyolite, cataclasite, and

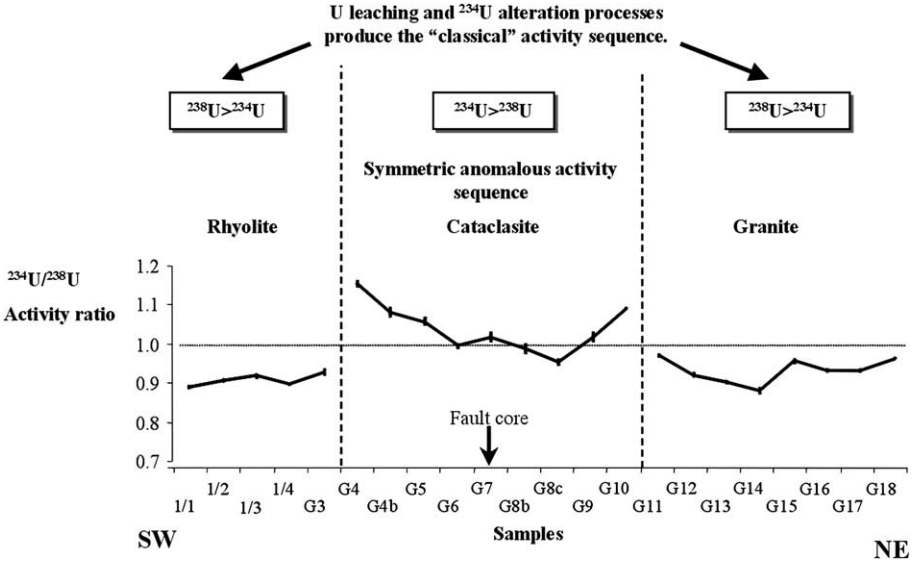


Fig. 2. Th/U disequilibrium profile. All the samples display a Th excess revealing that the samples have undergone uranium and thorium redistribution which occurred during the last $\sim 10^6$ years. The samples of the cataclasite record a more complex history of uranium exchange with the aqueous phase inducing a symmetrically distributed anomaly.

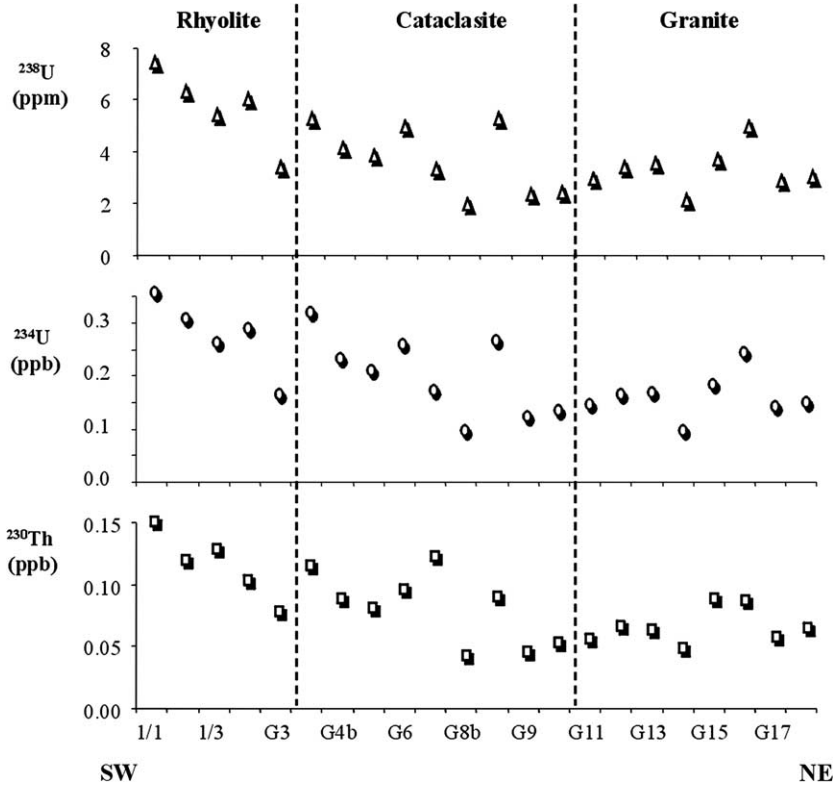


Fig. 3. Concentrations of $^{238}U$, $^{234}U$ and $^{230}Th$ across the Schauenburg profile. The concentrations show no trend across the sampled profile and no correlation with $\delta^{234}U$, suggesting an exchange with the aqueous phase without loss or sorption of uranium.

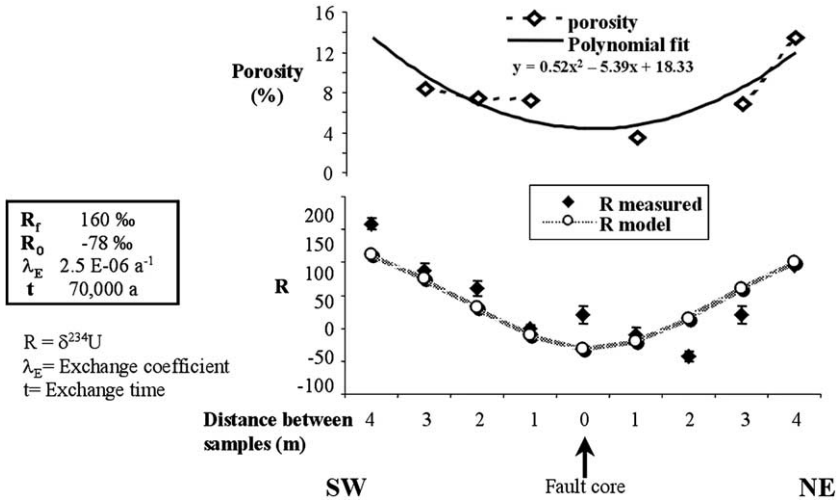


Fig. 4. Relation between porosity and uranium activity ratios for the cataclasite samples. This result is obtained assuming an exchange coefficient for uranium ranging from 2.5E−06 [$a^{-1}$] in the center of the cataclasite to 2.5E−05 [$a^{-1}$] along the walls of the cataclasite zone. The resulting exchange time for the approximation is 70 ka, which is considered to represent the age of the last alteration of the cataclasite samples.

granite). The rhyolite samples have a mean uranium content of 6 ppm and a relatively high mean thorium content of 38 ppm. These contents equal the highest range of values given for rhyolitic rocks in the literature. The granite and cataclasite rocks have a mean uranium content of 4 ppm, and a mean thorium content which is considerably lower (27 ppm and 17 ppm, respectively) than that of the rhyolite.

All the samples display excess $^{230}$Th ($^{230}Th_{exc} = {}^{230}Th - {}^{234}U$ in activities; Table 1) suggesting some redistribution of uranium and thorium has occurred within the last $\sim 10^6$ years. In the granite and rhyolite samples only uranium leaching (activity ratio $< 1$) has occurred. In contrast, cataclasite samples (G4–G10), with $^{234}U/^{238}U > 1$, record a more complex history of both sorption and loss of uranium (Fig. 2). In the cataclasite, the uranium activity ratios are higher ($1.020 < {}^{234}U/^{238}U < 1.158$) for the marginal samples collected close to the rhyolite and the granite (Fig. 2) and lower ($0.957 < {}^{234}U/^{238}U < 1.021$) for the samples situated in the middle of the cataclastically deformed zone. In contrast, the $^{238}$U-, $^{234}$U-, $^{230}$Th-concentrations (Fig. 3) and the $^{230}$Th excess (Table 1) do not show any trend across the sampled profile, and do not correlate with the uranium activity ratios.

The porosity measurements of the cataclasite samples show a pattern similar to the uranium activity ratios, with a symmetrical distribution across the core of the fault zone (Table 1 and Fig. 4). This distribution is characterized by higher porosity values (up to 13%) at the margins of the cataclastic zone and lower values (around 4%) towards the fault core. The latter values are similar to that measured on granite sampled further away from the fault.

## 5. Discussion

The symmetrical pattern of uranium activity ratios recognized across the cataclastic zone (samples G4 to G10) is characterized by an abrupt transition with the granite and rhyolite wall-rocks, where only uranium loss has occurred (Fig. 2). Contrastingly, $^{238}$U-, $^{234}$U-, $^{230}$Th-concentrations (Fig. 3) and the $^{230}$Th excess (Table 1) show no characteristic trends across the sampled profile, and thus do not correlate with the uranium activity ratios. Therefore the uranium activity ratio of the cataclasite cannot be explained only by sorption or loss of uranium but requires exchange with an aqueous phase having an activity ratio greater than 1 (Fig. 2). This is in contrast to the granite and the rhyolite samples, where uranium was leached (activity ratio $< 1$) but no exchange occurred with the aqueous phase.

The $^{234}U/^{238}U$ ratios along the profile, especially the symmetric anomaly recorded across the cataclasite zone, is suggested to correspond with the distribution of rock porosity (Fig. 4). Along the walls of the cataclastic zone, faulting and associated fracturing has led to an increase in the porosity (and presumably permeability) and thus enhanced contact between pore water and rock (i.e. a higher water–rock ratio). Therefore higher exchange of uranium isotopes with the aqueous phase can be predicted along the portions of the fault having a higher porosity, such as along the margins of the cataclastic zone, and restricted uranium isotopes exchange is expected in the zones of reduced porosity, namely in the core of the clay-rich cataclastic zone.

### 5.1. Exchange model

Using the U–Th and porosity data, we proposed a simple model to express the relationship between uranium isotopes exchange and the volume of pore space. The basic assumption of the model is that the change of the uranium activity ratios within the cataclasite mainly results from uranium isotopic exchange with the aqueous phase without

accumulation or leaching of uranium. The uranium activity ratio of the cataclasite equilibrates with the uranium activity ratio of the aqueous phase by exchange of uranium isotopes but without modification of the uranium global concentration. This assumption is considered to be valid because the uranium isotope concentrations of the cataclasite are not perturbed and do not correlate with the symmetrical distribution of the uranium activity ratios in the cataclasite.

In order to relate the porosity data with the $\delta^{234}U$ value, a simple exchange model was adopted from the study of uranium exchange in Mn-crusts by Neff et al. (1999). The model describes the $^{234}U$ variation in time in a solid phase (in this study the cataclasite) due to radioactive decay and exchange with a liquid phase (the pore water). The model can be applied for various natural systems by adapting the model parameters to the studied system.

The equation describing the behavior of the $\delta^{234}U$ (R) in rock due to radioactive decay of excess $^{234}U$ and to the exchange with pore water uranium is:

$$\frac{dR}{dt} = -(\lambda_E + \lambda_{234})R + \lambda_E R_f \quad (1)$$

The solution for Eq. (1) is :

$$R(t) = \left(1 - \frac{R_f}{R_0} \times \frac{\lambda_E}{(\lambda_E + \lambda_{234})}\right) R_0 e^{-(\lambda_E + \lambda_{234})t} + \frac{\lambda_E R_f}{(\lambda_E + \lambda_{234})} \quad (2)$$

Five parameters are involved in the equation: the $\delta^{234}U$ of the aqueous phase ($R_f$), the initial $\delta^{234}U$ of the rock ($R_0$), the decay constant of $^{234}U$ ($\lambda_{234}$), the exchange coefficient of $^{234}U$ incorporated in the rock with uranium dissolved in pore water ($\lambda_E$), and the time of exchange ($t$). The $\delta^{234}U$ of the aqueous phase (pore water) has been fixed ($R_f = 160‰$) to explain the highest $\delta^{234}U$ measured and matches well the range given for surface waters by Osmond and Cowart (1982). In surface waters, the $\delta^{234}U$ varies from nearly 100‰ to about 200‰. This range is smaller than found in ground waters because most surface waters are mixtures of runoff and diverse ground-water sources (Ivanovich and Harmon, 1992). The initial $\delta^{234}U$ values of the cataclasite samples ($R_0 = -78‰$) have been calculated by averaging the granite and rhyolite $\delta^{234}U$ values. The variable $\lambda_E$ and $t$ (respectively exchange coefficient of $^{234}U$ and exchange time) are then adjusted to fit the $\delta^{234}U$ of the model with the measured $\delta^{234}U$.

A higher porosity produces a greater $\lambda_E$ and therefore indicates more exchange reactions between the pore water and the rock. In all cases, the degree of isotopic alteration will be higher for the marginal samples of the cataclasite and lower in the fault core because of the symmetric pattern of porosity. The calculated $\lambda_E$ therefore reflects the degree of alteration which results from high water–rock interaction ratios (high $\lambda_E$) or low water–rock interaction ratios (low $\lambda_E$), respectively.

To evaluate the $\lambda_E$, the first step involves a polynomial fit of the porosity data for the cataclasite section ($y = 0.52x^2 - 5.39x + 18.33$, coefficient of determination $R^2 = 0.75$; Fig. 4). The obtained polynomial equation of the fit is then applied to the exchange coefficient of $^{234}U\lambda_E$ assuming a given $\lambda_E$ for the central sample ($\lambda_{E0}$):

$$\lambda_E = 0.52(\lambda_{E0})^2 - 5.39(\lambda_{E0}) + 18.33$$

Then with Eq. (2), the $\delta^{234}U$ for the cataclasite can be calculated. In doing so, we assume that for a given porosity a certain amount of uranium isotopes ($\delta^{234}U$ corresponding to the age of this layer) exchanges with pore water uranium isotopes. The rate of exchange controls both the steady state value (the second term of the equation) as well as the slope of the curve of the $\delta^{234}U$ (the exponent). The

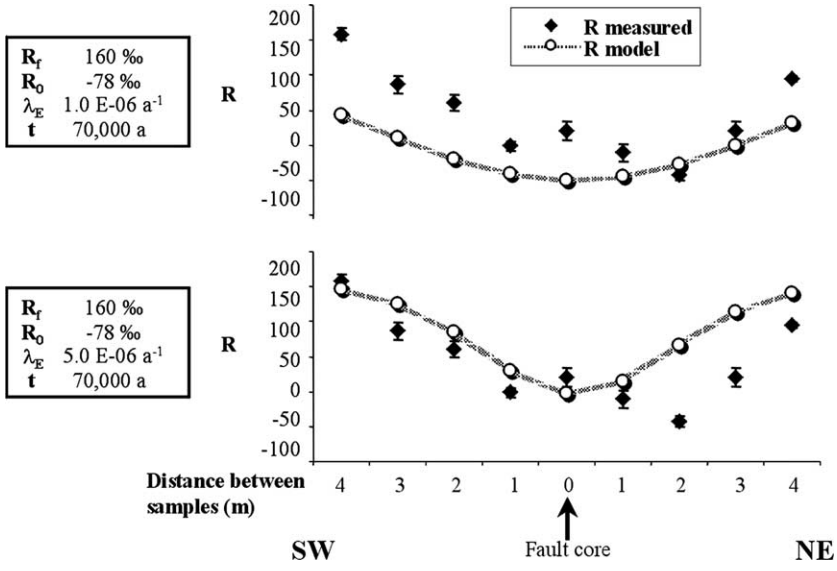


Fig. 5. Influence of various $\lambda_E$ values on the uranium activity ratios. The range for a suitable exchange coefficient is small. A lower $\lambda_E$ (1.0E−06 [$a^{-1}$]) produces less exchange with the aqueous phase. In this case, the sample has insufficient time to equilibrate with the aqueous phase. Using a higher $\lambda_E$ (5.0E−06 [$a^{-1}$]) results in a more rapid exchange with the aqueous phase.

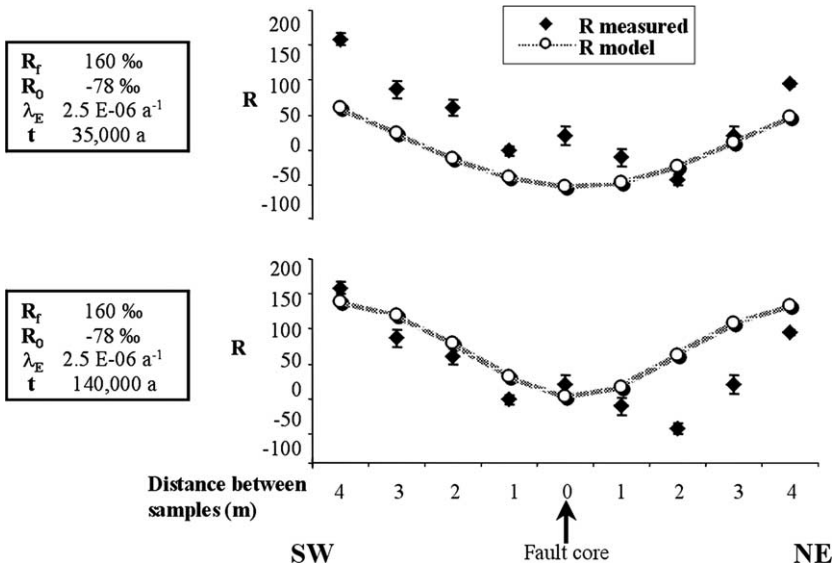


Fig. 6. Influence of various exchange times on the uranium activity ratios. Reducing the exchange time inhibits the samples ability to equilibrate with the aqueous phase. By increasing the exchange time of the model to 140 ka, the samples display more rapid exchange with the aqueous phase.

higher the rate of exchange, the flatter is the slope and the higher is the steady state value for $\delta^{234}U$.

The best approximation (using the statistical $\chi^2$ test, giving the best approximation for the lowest $\chi^2$) for the samples of the cataclasite is obtained by assuming an exchange coefficient for $^{234}U$ ranging from $2.5E{-}06a^{-1}$ for the core of the fault zone (given as start value for the model, Fig. 4) to $2.5E{-}05a^{-1}$ (calculated by the model for the fault walls). These values correspond to a residence time of absorbed uranium of 400 ka to 40 ka, respectively. The resulting exchange time for the approximation is 70 ka, which is suggested to represent the approximate age of the latest isotopic alteration within the Schauenburg fault. The trigger of this latest alteration event (of Pleistocene age) was possibly the last fault movement along this structure, related to the uplift of the Rhine Graben shoulder. During rupture of the fault zone, new waters could enter the fault associated with the formation of new fracture permeability. These waters subsequently could have been trapped during the growth of new authigenic clays within the pores of the cataclasite, leading to the reduction of porosity recognizable in the central fault core.

Also shown is the sensitivity of the calculated $\delta^{234}U$ values when various exchange coefficients of $1.0E{-}06a^{-1}$ and $5.0E{-}06a^{-1}$ are used for the central fault sample (Fig. 5). This relationship indicates that the range of suitable values for the exchange coefficient is small. A lower $\lambda_E$ ($1.0E{-}06a^{1}$) value indicates less exchange with the aqueous phase. A similar effect can be obtained by reducing the exchange time of the model to 35 ka (Fig. 6). However in this case, the sample would not have had sufficient time to equilibrate with the aqueous phase. Using a higher $\lambda_E$ ($5.0E{-}06a^{-1}$), leads to more rapid exchange with the aqueous phase, which can also be attained by increasing the exchange time of the model to 140 ka (Fig. 6). A similar study of uranium exchange coefficients in igneous rocks has is not yet been reported to our knowledge, and therefore a comparison with other data is not possible.

## 6. Conclusions

The exchange rate of absorbed uranium isotopes across the Schauenburg fault zone, positioned along the uplifted shoulder of the Rhine Graben rift, is related to the distribution of pore space. Differences in the pore volume can be related to the increase and reduction of fracture permeability during fault activity and subsequent authigenic clay mineral growth. Along the outer core of the cataclastic fault zone, the enhanced porosity, and thus permeability, resulted in prolonged contact between water and rock. Here, a higher exchange of uranium isotopes with the aqueous phase occurred. Within the core of the fault, the porosity is lower and the availability of circulating fluids restricted the exchange of uranium isotopes between the rock and the aqueous phase. A best approximation is reached using an exchange coefficient ($\lambda_E$) for $^{234}U$ ranging from $2.5E{-}06a^{-1}$ in the fault core to $2.5E{-}05a^{-1}$ in the fault walls (Fig. 4).

Application of the exchange model provides some general constraints for the age of uranium isotopic exchange and thus the age of the last significant event of fluid–rock interaction. The Pleistocene date of ca. 70 ka is suggested to reflect a young stage of the faults history characterized by significant fluid activity, which was possibly triggered by fault reactivation of this structure during uplift of the Rhine Graben shoulder.

## Acknowledgements

This paper forms part of the doctorate study of Thierry Marbach, which was conducted within the framework of the GRK 273 programme on fluid–rock interaction, funded by the DFG (german research council). Fabrice

Surma (EOST Strasbourg) is thanked for conducting the porosity measurements.

## References


Batzle, M.L., Simmons, 1977. Geothermal systems: rocks, fluids, fractures. Am. Geophys. Union Monogr. 20, 233–242.

Bollhöfer, A., Eisenhauer, A., Frank, N., Pech, D., Mangini, A., 1996. Th- and U-isotopes in a Mn-nodule from the Peru Basin determined by alpha spectrometry and thermal ionisation mass spectrometry: are manganese supply and growth related to climate? Geol. Rundschau. 85, 577–585.

Caine, J.S., Evans, J.P., Forster, C.B., 1996. Fault zone architecture and permeability structure. Geology 24, 1025–1028.

Chen, J.H., Edwards, R.L., Wasserburg, G.J., 1986. $^{234}U$, $^{238}U$ and $^{232}Th$ ibn seawater. Earth Planet. Sci. Lett. 80, 241–251.

Chester, F.M., Evans, J.P., Biegel, R.L., 1993. Internal structure and weakening mechanisms of the San Andreas Fault. J. Geophys. Res. 98, 771–786.

Edwards, R.L., Beck, J.W., Burr, G.S., et al., 1993. A large drop in atmospheric $^{14}C/^{12}C$ and reduced melting in the Younger Dryas, documented with $^{230}Th$ ages of corals. Science 260, 962–968.

Eisenhauer, A., Wasserburg, G.J., Chen, J.H., et al., 1993. Holocene sea-level determination relative to the Australian continent: U/Th (TIMS) and $^{14}C$ (AMS) dating of coral cores from the Aborlhos Islands. Earth Planet. Sci. Lett. 114, 529–547.

Frank, N., 1997. Anwendung der Thermionen Massenspektrometrie zur Uranreihen Datierung von pleistozäne mitteleuropäischen Travertinen. Ph.D. Thesis, University of Heidelberg.

Harmon, R.S., Thompson, P., Schwarcz, H.P., Ford, F.C., 1975. Uranium-series dating of speleotherm. Nat. Spel. Soc. Bull. 37, 21–33.

Hess, J.C., Lippolt, H.J., 1996. Numerische Stratigraphie permokarbonischer Vulkanite Zentraleuropas. Teil III: Odenwald. Geol. Jb Hessen. 124, 39–46.

Hooper, E.C.D., 1991. Fluid migration along growth faults in compacting sediments. J. Petroleum Geol. 14, 161–180.

Ivanovich, M., Harmon, R.S., 1992. Uranium-series Disequilibrium, 2nd ed. Oxford Science Publications, 899.

Kaufman, A., Broecker, W.S., Ku, T.-L., Thurber, D.L., 1971. The status of U-series methods of dating mollusks. Geochim. Cosmochim. Acta 35, 1155–1183.

Kunzendorf, H., Friedrich, G.H.W., 1976. The distribution of U and Th in growth zones of manganese nodules. Geochim. Cosmochim. Acta 40, 849–852.

Lippolt, H.J., Kisch, H., Plein, E., 1990. Karbonische und permische Vulkanite aus dem Untergrund des nördlichen Oberrheingrabens: Art, Alterbestimmung und Konsequenz. Jber. Mitt. Oberrhein. Geol. 72, 227–242.

Marbach, T., 2002. Fluid–rock interaction history of a faulted rhyolite–granite contact, eastern Rhine graben shoulder, SW Germany: alteration determined by Sr–Pb-isotopes, Th/U disequilibria and elemental distributions. Doctorate Thesis, University of Heidelberg, p. 140.

Neff, U., Bollhöfer, A., Frank, N., Mangini, A., 1999. Explaining discrepant depth of $^{234}U/^{238}U$ and $^{230}Th_{exc}$ in Mn-crusts. Geochim. Cosmochim. Acta 63, 2211–2218.

Osmond, J.K., Cowart, J.B., 1982. Ground water. In: Ivanivich, M., Harmon, R.S. (Eds.), Uranium Series Disequilibrium: Applications to Environmental Problems, first ed., pp. 202–245.

Power, W.L., Tullis, T.E., Brown, S., Boitnott, G.N., Scholz, C.H., 1987. Roughness of natural fault surfaces. Geophys. Res. Lett. 14, 29–32.

Rogers, J.J.W., Adams, J.A.S., 1969. Uranium. In: Wedepohl, K.H. (Ed.), Handbook of Geochemistry. Springer Verlag, Berlin.

Schleicher, A., 2001. Niedrig temperierte Alterationsprodukte in felsischen Gesteine am Beispiel der Schauenburgstörung, östliche Rheingrabenschulter bei Heidelberg, Diplomarbeit, p. 115.

Schleicher, A.M., Warr, L.N., van der Pluijm, B.A., 2005. Fluid focusing and back-reactions in the uplifted shoulder of the Rhine rift system: a clay minerals study along the Schauenburg fault zone (Heidelberg, Germany). Int. J. Earth Sci., in press, doi:10.1007/s00531-005-0490-3.

Sibson, R.H., 1994. Crustal stress, faulting and fluid flow. Geol. Soc. Special Publ. 78, 69–84.

Smith, D.A., 1980. Sealing and non sealing faults in Louisiana Gulf Coast Salt Basin. Am. Assoc. Petroleum Geol. Bull. 64, 145–172.

Sturchio, N.P., 1994. Uranium-series ages of Travertines and timing of the Last Glaciation in the Northern Yellowstone Area, Wyoming-Montana. Quarter. Res. 41, 265–277.

Surma, F., Géraud, Y., 2003. Porosity and thermal conductivity of the Soultz-Sous-Forêts granite. Pure Appl. Geophys. 160 (5–6), 1125–1136.

Vrolijk, P., van der Pluijm, B.A., 1999. Clay gouge. J. Struct. Geol. 21, 1039–1048.